

Surface Figure Measurement at 80K: Alignment and Uncertainty Analysis

Peter Blake^{*a}, Ronald G. Mink^a, John Chambers^a, Pamela Davila^a,
David Content^a, F. David Robinson^{a,b},

^a Goddard Space Flight Center, Code 551, Greenbelt, MD 20771

^b Orbital Sciences Corporation, 7500 Greenway Center Drive, Suite 700, Greenbelt MD 20770

1. INTRODUCTION

The Optics Branch of the Goddard Space Flight Center (GSFC), interested in staying abreast of the rich, almost explosive development in new materials and forms for lightweight space-based astronomical mirrors, is developing its interferometry capabilities to new levels of precision. This paper presents our progress to date on the high-precision cryogenic facility. The facility is baselined for spherical mirrors with a radius of curvature (ROC) of 600 *mm*, and a clear aperture of 120 -- 150 *mm*. Our goal is to achieve uncertainties of 3 *nm rms* in the measurement at 20K of mirrors with a specified surface figure error (SFE) of 10 *nm rms*.

The near-term goals of the currently-reported experiment were:

- 1) Obtain the best possible estimates of the test mirror surface figure error (SFE) at both ambient conditions (room temperature) and at cryogenic temperatures. By SFE, we are referring to the two-dimensional map of deviation from the best-fit sphere; and we use the terms figure, surface figure, surface figure error, and error map synonymously.
- 2) Determine the uncertainty of these measurements.

2. TEST MIRROR AND TEST CONDITIONS

The first mirror tested was a flat-backed silicon foam-core mirror, concave spherical with radius of curvature of 600 *mm*, a thickness of 17.4 *mm*, and a clear aperture of 120 *mm*. The mirror was made by the Schafer Corporation in 2001, and is an early example of their SLMSTTM technology¹.

To assure the highest possible accuracy and precision, it was decided that there would be no sources of mechanical strain introduced into the mirror by differential thermal contractions in the mount or in the heat strapping. The mirror would be simply-supported on two support points, with its flat back resting against the cold plate (fig. 1). There would be no constraint of the mirror and no thermal straps connected to the mirror.

The cold plate and inner shroud, which surround the mirror, except for the aperture, can be lowered to 12K with liquid helium. But with no heat straps and no thermal medium joining the mirror to the cold plate – just the three points of contact – the temperature performance of the mirror was unknown. Since radiative heat transfer scales as the fourth power of absolute temperature, once the mirror temperature falls below about 100K, the cooling of the mirror was expected to be slow, and would be countered by the small amount of radiation coming from the window at room temperature. As it turns out, the mirror reached a temperature of 95K with liquid nitrogen and 80K with liquid helium.

3. FACILITY

The test facility for cryo-measurement of the prototype mirrors was described in an earlier paper by these authors². A Zygo “Verifire AT”[®] phase measuring interferometer, positioned on crossed rails, focuses through a window into a cryostat or dewar. The cryostat has tip/tilt controls. The whole facility rests on a curtained vibration isolation table.

* peter.n.blake@nasa.gov; phone 301 286-4211; fax 301 286-0204

A simple design feature takes advantage of the converging interferometer beam for the testing of a 600 mm ROC sphere. We are able to use a small window and place it close to the focal point of the interferometer (figure 2) using a cylindrical extension that has been placed over the original window. There are several significant advantages: a) a small window can be thinner for a given deflection under vacuum, leading to less spherical aberration; b) a small footprint of the beam on the window makes it easier to achieve low transmitted wavefront error (WFE); and c) placing the window 600mm from the mirror on a narrow extension cylinder lowers the radiative coupling between the mirror and the window, lessening the mutual distortions of the window and the mirror.

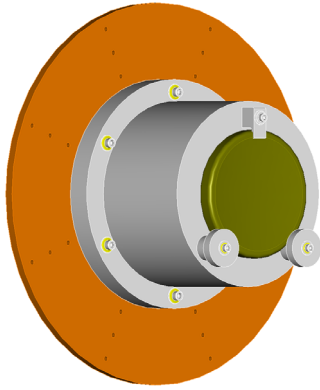


Fig 1: SLMS mirror supported on cold plate

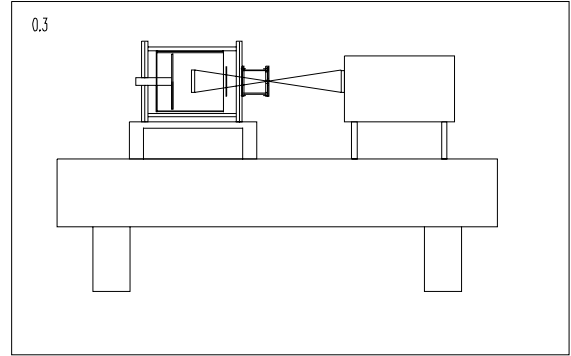


Fig 2: Dewar with window and snout added

4 CORRECTION OF SYSTEMATIC EFFECTS

As will be seen in the discussion of uncertainty analysis, we confined our search for and correction of systematic effects to those whose contribution to the SFE measurement was greater than 0.4 nm rms.

The primary systematic effect that requires correction is the aberration of the beam as it passes twice through the window of the cryostat. This aberration has been modeled using the software program Zemax®, as described in a previous paper². It was found that if the optic axis were perpendicular to the window of the cryostat, the only aberration that contributed an SFE error of greater than 0.4 nm rms was spherical aberration, which contributed an error of 8.8 nm rms. It was found, however, that if the window were tilted, not only were there added contributions of coma and astigmatism, but the amount of aberration depended on the distance of the mirror from the window. Since this distance could change during thermal excursions, without our having any way to measure it, it was determined to keep the angle of the optic axis to the window less than 0.4 arcmin, giving an error of approximately 0.4 nm rms over and above the aberration at perpendicularity.

The window aberrations can be removed by two different calculations: 1) by subtracting the modeled or calculated aberrations from the final measured SFE; and 2) by measuring the change in SFE that occurs with the test mirror in the cryostat – behind the window – as the temperature drops from RT to cryogenic temperature (80K). When the measurement at room temperature and vacuum is subtracted from the measurement at 80K, the window aberrations of the two measurements -- shown by modeling to differ by less than 0.1 nm rms² – are eliminated.

The method chosen should be the method with the least uncertainty. Our baseline approach, which is the only approach reported here, is the second: finding the change upon cooling (the “cryo-deformation” or the “cryo-difference map”) and adding this to the unwindowed room temperature (“ambient”) surface figure error.

In the interferometer itself, the only systematic effect above 0.4 *nm rms* is imperfection of the reference surface in the transmission sphere. This error can be measured and subtracted by a technique called “absolute measurement” or the “two-sphere test”³. This technique will give both a corrected map of the test mirror SFE and a map of the interferometer errors over the pupil. This map of the interferometer error can be used as an error file to correct the measurements of test mirrors that do not lend themselves to the two-sphere test. For example, the ESA mirrors to be measured soon in our lab have integral feet for mounting, and would not be suitable for the two-sphere test, since gravity would force variations in surface figure as the mirror was rotated.

5 UNCERTAINTY DEFINED

Consider a result of an optical test W , which is an estimate of a surface figure. The result W is a set of N data points $\{w_1, w_2, \dots, w_n\}$ over a two-dimensional array. This measurement is the sum of the true surface figure error S , several contributions of systematic effects, and several contributions of statistical noise⁴. We will make efforts to remove the systematic effects, as described in section 4, but each correction has itself an unknown error, which must be estimated. The terminology becomes much clearer when we adopt the conception of *uncertainty*, as defined by NIST and ISO⁵:

“Basic to the [ISO] approach is representing each component of uncertainty that contributes to the uncertainty of a measurement result by an estimated standard deviation, termed standard uncertainty, with suggested symbol u_i ...”

An uncertainty component, then, can be statistically determined – the statistically estimated standard deviations s_i , and the associated number of degrees of freedom ν_i ; or it may be approximated: “obtained from an assumed probability distribution based on all the available information.”

“The **combined standard uncertainty** of a measurement result, suggested symbol u_c , is taken to represent the estimated standard deviation of the result. It is obtained by combining the individual standard uncertainties u_i (and covariances as appropriate)...using...the *law of propagation of uncertainty*, the “root-sum-of squares”...or “RSS” method of combining uncertainty components estimated as standard deviations....”

It is assumed that a correction (or correction factor) is applied to compensate for each recognized systematic effect that significantly influences the measurement result and that every effort has been made to identify such effects. The relevant uncertainty to associate with each recognized systematic effect is then the standard uncertainty of the applied correction.”

Our task, then, is to estimate every individual uncertainty component, and sum them in quadrature.

5.1 Metrology goals

Our goal is to measure the cryo-figure of mirrors with specified SFE’s of $< 10 \text{ nm rms}$. Since a system level requirement for wavefront errors (WFE) is the sum in quadrature of the individual optic wavefront errors, and since it would be a reasonable goal to limit the uncertainty of the system-level WFE to 10%, the uncertainty goal for an individual measurement would be $\sqrt{0.1} \approx 0.3$, or 3 nm rms .

With an uncertainty goal of 3 nm rms , we limited our search to uncertainty components that were equal to or greater than 0.4 nm rms ; since ten such uncertainties, added in quadrature to other sources totalling 3 nm rms , would increase the total uncertainty of the optic by less than 10%.

5.2 Uncertainty as a root mean square

The root mean square (rms) of the surface deformation is a quantitative measure of the quality and performance of an optic, and, as such, is the final figure of merit in many investigations.

But how do we speak of the uncertainty of the surface figure itself – not the uncertainty of the rms figure, but the uncertainty of the two-dimensional map which is our estimate of the surface? The measurements, the corrections, and the final estimate of SFE are all maps over two dimensions. The uncertainties are not maps, *per se*, because they are unknown; but they are two-dimensional.

An approach has been suggested Ulf Griesmann, NIST⁶. The reported SFE is the sum of the true surface figure error S and unknown error. This error, although unknown, has an rms value. Our estimate of the expected range for rms value of the error is what we shall call the uncertainty of the measurement.

For example, following Griesmann, the short-term statistical component of uncertainty can be estimated by the following procedure:

- a Make multiple identical measurements (e.g., twenty times).
- b Average the multiple plots.
- c Subtract the mean plot – pixel by pixel -- from each measurement, to form what we'll call a delta.
- d Calculate the rms deviation of each of the deltas.
- e Determine the distribution of the rms values of the deltas: e.g., plot a histogram of frequency vs. rms; find the mean of the distribution and the standard deviation, s .
- f The uncertainty of the multiple measurements is defined such that 68% of the rms values are smaller than the uncertainty (68% confidence level analogous to the standard deviation). Thus uncertainty = mean + 0.468 * s .

Because our interest is often in the surface figure itself, or in the power spectral density, we will carry through all computations of uncertainty as computations of the uncertainty of the surface figure, not uncertainty of the rms value itself, which can be calculated at the end.

6 MEASUREMENTS

Temperatures inside the dewar and in the test mirror were measured with temperature-sensing diodes. In order to limit the thermo-mechanical strain caused by attachment of diodes to the optic, the diodes were wired with 42 gage copper and attached to the mirror edge with a thin layer of GE Varnish.

When the cold plate was held at liquid nitrogen (77K), the mirror cooled down to 95K. When the cold plate was held at liquid helium temperature, the mirror cooled only to 80K. Our criterion for sufficient temperature stability for measurement was that the rate of change of the mirror fall below 1K/15 min.

The mirror was subjected to three thermal cycles, with measurements taken at the following points:

RTP: ambient conditions, room temperature, no window, no vacuum

RTV: Measurement taken through the window. Test mirror in dewar at room temperature under vacuum.

95K: Cold plate at liquid nitrogen temperature, mirror at 95K

80K: Cold plate at liquid helium temperature, mirror at 80K

When the rate of cooling was 1K/hr, the shutter was opened and the radiation from the window halted the cooling. On opening the shutter, the image is nulled and the measurement taken, as the mirror rises in temperature at close to 2K/hr.

For each measurement step of the thermal cycle, twenty successive individual measurements were taken, each using thirty-two phase averages.

7 RESULTS

In the cryo-cycling trials reported here, our correction for the error of the reference surface was to subtract the matching portion of the Zygo error file. The resultant SFE at 90% CA was found to be 22.6 *nm rms*.

Both systematic errors – window aberration and reference surface error -- are subtracted out when the data file for the mirror in the dewar, in vacuum at room temperature (RTV) is subtracted from the data file for the mirror at 80K, after registering the files as closely as possible. The result was a cryo-change difference map with an rms of 4.9 *nm rms*. When the cryo-change difference map is added to the ambient condition measurement (corrected for reference surface error) the result --- SFE at 80K -- has an RMS of 25.0 *nm*.

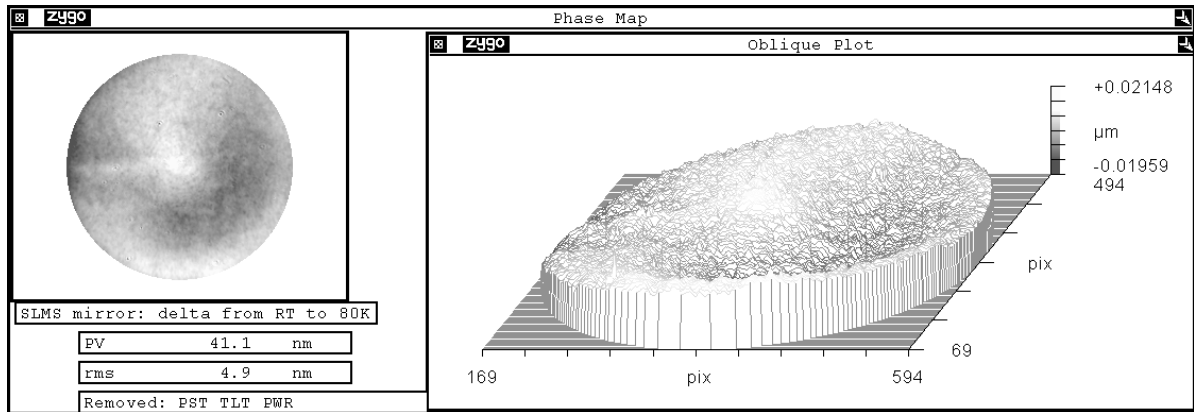


Figure 3: Change on Cooling of Schafer mirror

8 UNCERTAINTY ANALYSIS

8.1 Short-term statistical Uncertainty

When the twenty individual measurements are averaged, and the deviation of each measurement is subtracted from the mean, the short-term variation can be measured:

- at RTP, the short-term statistical uncertainty is: 0.7 nm rms
- at RTV, the short-term statistical uncertainty is: 0.9 nm rms
- at 95K, the short-term statistical uncertainty is: 0.8 nm rms
- at 80K, the short-term statistical uncertainty is: 1.2 nm rms

The higher uncertainty at 80K was reflected in the measurements themselves: in the drop-out of pixels from the top edge of the optic: indicating a vibratory wobbling of the whole optic on its support. These parameters represent uncertainties of the individual measurements, and include some OPD arithmetic uncertainty (see below). The mean of all twenty measurements for a condition would have an even lower uncertainty. We take $\frac{1.2nm}{\sqrt{20}}$ to be a reasonable estimate of the short-term statistical contribution.

8.2 Long-term statistical Uncertainty

A measure of the long-term statistical uncertainty was made in a previous experiment², and was found to contribute (in RSS) an additional 0.8 nm rms to the statistical uncertainty.

8.3 Arithmetic Uncertainty

For each individual addition or subtraction of wavefronts (called OPD or *optical path length* arithmetic), a good estimate can be made of the uncertainty of position of the sets – the uncertainty of registration and congruence, pixel-for-pixel. The resultant error in the SFE stemming from that degree of misregistration can be quickly determined by taking an individual measurement, translating or mis-aligning it by that degree and subtracting it from the original. This estimation was done for every such addition or subtraction of data sets, with the calculated uncertainties ranging between 0.5 nm rms and 1.7 nm rms.

8.4 Optic Axis Alignment Uncertainty

Our technique for aligning the optic axis to the dewar window⁷ was accurate to within one pixel of the camera, which translates to an uncertainty of 0.4 nm rms.

8.5 Uncertainty of error file

To produce the error file used by us (4.4 nm rms), the Zygo corporation used a two-sphere test of the transmission sphere in our interferometer. We found it best to characterize this transmission sphere error by the first 36 Zernikes of the measured error file, losing the residual. This loss of the residual adds an additional uncertainty of 1.3 nm.

There is also uncertainty in the error file itself, which we estimated by examining the difference between two independent measurements: Zygo's measurement (using a convex mirror in a short cavity) and our own two-sphere measure of the transmission sphere, using the test mirror in the same cavity as is used in measuring the test mirror. The use of test mirror suffers the sole flaw of not filling the pupil. Over the common portion of the pupil, the two measurements differed by 1.4 nm rms, an amount that could be due to short-term and OPD arithmetic uncertainty; but 1.4 nm was taken as a conservative estimate of the reference surface uncertainty.

If when the two measurement files for 80K and RTV are subtracted, the two files do not occupy the same space in the pupil, there is small error contributed by the shear of the error file. This error is smaller than the OPD arithmetic necessary to eliminate it, so the uncertainty of the OPD arithmetic was conservatively assigned to this factor.

8.6 Combined Standard uncertainty

Combining these uncertainties in standard RSS form, with individual contributions from each iteration of OPD arithmetic, gives us an uncertainty in our map of cryo-deformation of 2.2 nm rms.

It is tempting to add and subtract in quadrature the estimated uncertainty of 2.2 nm rms with the estimated cryo-deformation of 4.9 nm rms in order to obtain an "error bar" between 4.4 nm and 5.4 nm rms for the surface figure RMS parameter. This does not appear to be legitimate, because several contributions to the uncertainty, such as the OPD arithmetic, are clearly not independent of the surface figure, and may be correlated with the cryo-deformation also.

More study of the propagation of uncertainty through these calculations is warranted.

ACKNOWLEDGEMENTS

The authors gratefully acknowledge the assistance of the Schafer Corporation, the European Space Agency, and the James Webb Space Telescope. Our thanks also to Chip Frohlich and Badri Shirgur of the Swales Corporation, Beltsville MD, and to Joe McMann of Mantech Systems Engineering Corp., Greenbelt, for their expert assistance on many aspects of this program. Special Thanks to Ulf Griesmann, NIST, for valuable discussions.

Mention of trade names or commercial products does not constitute endorsement or recommendation by NASA.

REFERENCES

- ¹ Marc T. Jacoby, *et. al.*, "Helium cryo-testing of a SLMS™ (silicon lightweight mirrors) athermal optical assembly, *Proc SPIE 5180, Optical Manufacturing and Testing V*, ed. Phil Stahl, pp199-210, 2003
- ² P. Blake, R. G. Mink, D. Content, P. Davila, F. D. Robinson, S. R. Antonille, "Techniques and uncertainty analysis for interferometric surface figure error measurement of spherical mirrors at 20K", *Proc SPIE, 5180, Optical Manufacturing and Testing V*, ed. Phil Stahl, pp188-198, 2003.
- ³ K. Elssner, R. Burow, J. Grzanna, R. Spolaczyk, "Absolute Sphericity Measurement," *Applied Optics*, **28**, pp 4649-4661, 1989
- ⁴ A. Davies, M.S. Levenson, "Estimating the root mean square of a wave front and its uncertainty", *Applied Optics*, **40**, pp 6203-6209, 2001
- ⁵ B. Taylor, C.E. Kuyatt, "Guidelines for Evaluation and Expressing the Uncertainty of NIST Measurement Results", NIST Technical Note 1297, 1994
- ⁶ Ulf Griesmann, National Institute of Standards and Technology, Gaithersburg, MD, personal communication.
- ⁷ To be published in *NASA Tech Briefs*